

Supplementary information

Nanoscale liquid Al phase formation through beam heating of MgAl_2O_4 in TEM

Sung Bo Lee*, Jun Young Chae, Heung Nam Han

Department of Materials Science and Engineering and Research Institute of Advanced
Materials, Seoul 08826, Republic of Korea

*Corresponding author. bole@snu.ac.kr (S.B.L.)

Table S1. Compositions of elements in MgAl_2O_4 (in at. %), measured from the boxes drawn in the unirradiated matrix and the irradiated region in Fig. 2b.

	Matrix	Irradiated
O	54.9	23.4
Mg	14.2	7.3
Al	30.9	69.3

Table S2. Concentration of Ga measured by Scanning TEM-energy dispersive X-ray spectroscopy (EDXS), obtained from the boxed area in the irradiated region (Fig. S1).

Element	O	Mg	Al	Ga
Atomic fraction (%)	33.57	6.05	60.24	0.14

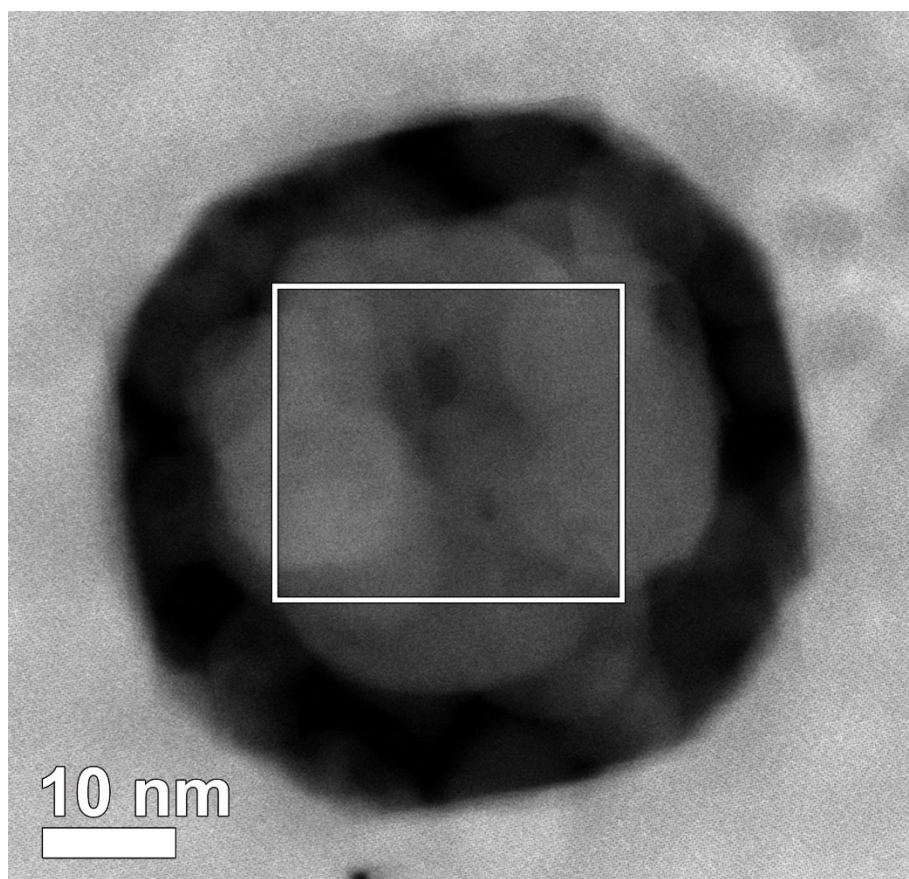


Fig. S1. High-angle annular dark-field (HAADF) image taken at the end of the irradiation, acquired with a probe diameter of 80 pm and a dwell time of 2 μs .

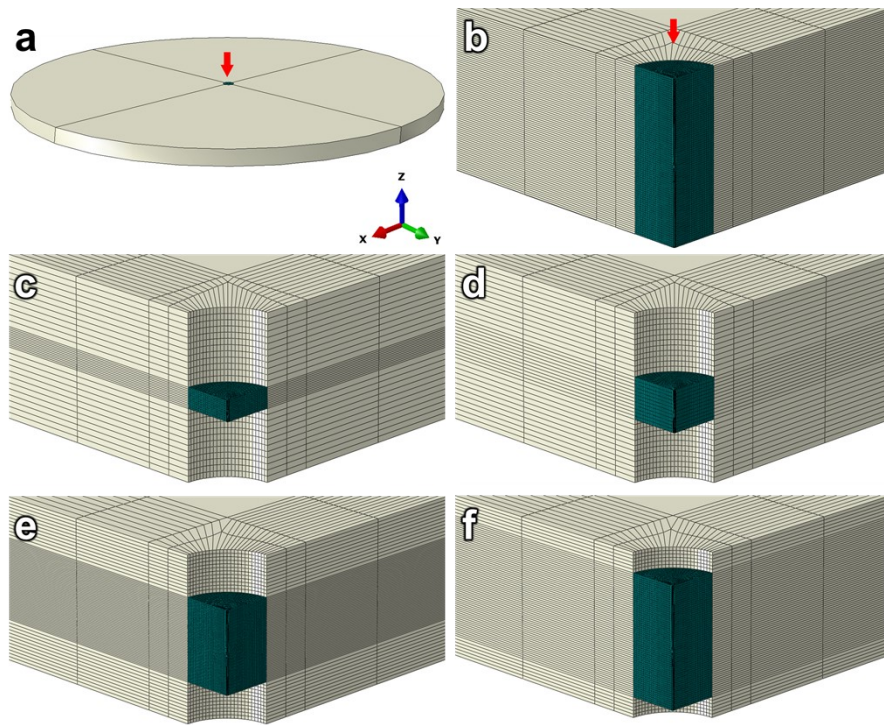


Fig. S2. (a) A full geometric representation of the 50-nm-diameter irradiated region at the center of a 2- μm -diameter, 80-nm-thick sheet. (b) to (f) Enlarged views of quarter-symmetric FE models of the irradiated region, highlighted in dark green, with thicknesses of 80, 60, 40, 20, and 10 nm, respectively.

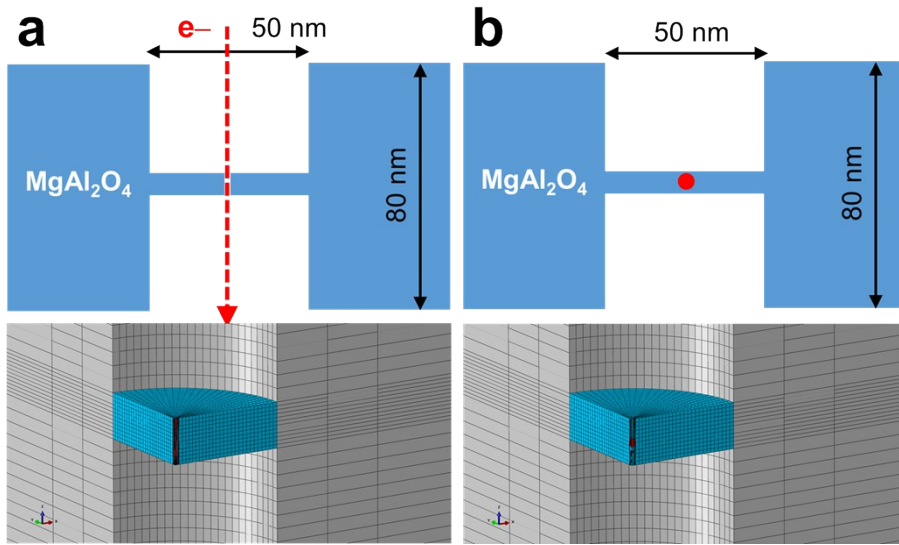


Fig. S3. Illustrations showing different heat source arrangements. (a) A cross-section showing energy deposition due to the energy-loss effect, with a schematic finite element (FE) model showing the heat source as a red line. (b) A cross-section showing energy deposition due to the Auger effect, accompanied by a corresponding schematic FE model in which the heat source is represented as a red dot 2 nm in diameter. Note that the energy of an electron is intended to be deposited precisely at the center of the MAO layer.

Table S3. Input thermal conductivities (in $\text{W m}^{-1} \text{K}^{-1}$) for the irradiated region with varying thicknesses of MAO.

Thickness (nm)	10	20	40	60	80
Cross-plane, lower/upper (z)*	3.7/6.4	4.7/7.3	5.4/8.1	5.9/8.4	6.1/8.7
In-plane (x, y)	8.7	8.7	8.7	8.7	8.7

*The cross-plane data are adapted from Negi et al.,¹ while the bulk thermal conductivity measured at 300 K² is for the in-plane data.

1. Derivation of the deposited energy in the MAO layer for the Auger effect

We use a weighted average formula to obtain the average deposited energy. For Mg, its Auger energy (1188 eV)³ is multiplied by the product of the cross section for K-shell ionization in Mg ($2.7 \times 10^{-21} \text{ cm}^2$)⁴ and the number of Mg atoms in the formula unit (1 in MgAl₂O₄), yielding ($1188 \times 2.7 \times 10^{-21} \times 1$). The same procedure also applies to Al and O,^{3,4} yielding ($1396 \times 2 \times 10^{-21} \times 2$) for Al and ($510 \times 7.5 \times 10^{-21} \times 4$) for O.

Dividing the sum of these products by the sum of the products of the cross sections and the number of atoms in the formula unit results in the weighted average deposited energy:

$$\frac{(1188 \times 1 \times 2.7 + 1396 \times 2 \times 2 + 510 \times 4 \times 7.5)}{(1 \times 2.7 + 2 \times 2 + 4 \times 7.5)} = 656.45 \text{ eV},$$

where the exponential notation (10^{-21}) is omitted for simplicity.

2. Input energies for the Auger effect in FEA

The inelastic mean free path (IMFP) of electrons in a nanometer-thick film of thickness (t) is considered. Assuming that inelastic scattering and surface scattering occur independently, the effective electron mean free path (IMFP) in the nanometer-thick film (λ_f) is calculated using Matthiessen's rule:^{5,6}

$$1/\lambda_f = 1/\lambda + 1/t.$$

Here, λ is the IMFP in the bulk counterpart. $1/\lambda_f$ indicates the total number of scattering events per unit distance, while $1/\lambda$ represents the number of inelastic scattering events per unit distance. The probability of inelastic scattering in the nanofilm is given by p :

$$p = \lambda_f/\lambda = t/(\lambda + t)$$

Taking into account the Auger 656.45-eV electron, which has an IMFP of 1.814 nm corresponding to λ ,⁷ for $t = 80$ nm, p is ~ 0.98 , resulting in an estimated deposited energy of 641.90 eV. The results obtained by applying the above expression to all the thicknesses examined are detailed in Table S4.

Table S4. Input energy parameters due to the Auger effect (in eV) for the irradiated region with varying thicknesses of MAO.

Thickness (nm)	10	20	40	60	80
Auger	555.65	601.86	627.97	637.19	641.90

Table S5. Atom counts for each element and corresponding time intervals between Auger events for MAO layer thicknesses of 10 nm and 80 nm (in seconds).

MAO thickness (nm)	Mg atoms	Al atoms	O atoms	Time for Mg	Time for Al	Time for O
80	2,382,187	4,764,373	9,528,747	1.2×10^{-7}	8.3×10^{-8}	1.1×10^{-8}
10	297,773	595,547	1,191,093	9.8×10^{-7}	6.6×10^{-7}	8.8×10^{-8}

References

1. A. Negi, A. Rodriguez, X. Zhang, A. H. Comstock, C. Yang, D. Sun, X. Jiang, D. Kumah, M. Hu and J. Liu, Thickness- dependent thermal conductivity and phonon mean free path distribution in single-crystalline barium titanate, *Adv. Sci.*, 2023, **10**, 2301273.

2. C.-M. Ni, H.-W. Fan, X.-D. Wang and M. Yao, Thermal conductivity prediction of MgAl_2O_4 : a non-equilibrium molecular dynamics calculation, *J. Iron Steel Res. Int.*, 2020, **27**, 500–505.
3. K. D. Childs, B. A. Carlson, L. A. LaVanier, J. F. Moulder, D. F. Paul, W. F. Stickle and D. G. Watson, edited by C. L. Hedberg, Handbook of Auger Electron Spectroscopy: A Book of Reference Data for Identification and Interpretation in Auger Electron Spectroscopy, 3rd Ed. (Physical Electronics, Inc., Eden Prairie, MN, 1995).
4. X. Llovet, F. Salvat, D. Bote, F. Salvat-Pujol, A. Jablonski and C. J. Powell, NIST Database of Cross Sections for Inner-Shell Ionization by Electron or Positron Impact, Version 1.0, SRD 164 (National Institute of Standards and Technology, Gaithersburg, Maryland, 2014).
5. Z. M. Zhang, Nano/Microscale Heat Transfer, 2nd Ed., Springer Nature, Cham, Switzerland, 2020, Chap. 5.
6. P. Warriar and A. Teja, Effect of particle size on the thermal conductivity of nanofluids containing metallic nanoparticles, *Nanoscale Res. Lett.*, 2011, **6**, 247.
7. C. J. Powell and A. Jablonski, NIST Electron Inelastic-Mean-Free-Path Database- Version 1.2, SRD 71 (National Institute of Standards and Technology, Gaithersburg, MD, 2010).